Mast cell–expressed orphan receptor CCRL2 binds chemerin and is required for optimal induction of IgE-mediated passive cutaneous anaphylaxis

Brian A. Zabel,[1] Susumu Nakae,[2] Luis Zúñiga,[1] Ji-Yun Kim,[1] Takao Ohyama,[1] Carsten Alt,[1] Junliang Pan,[1] Hajime Suto,[2] Dulce Soler,[3] Samantha J. Allen,[4] Tracy M. Handel,[4] Chang Ho Song,[2,5] Stephen J. Galli,[2,6] and Eugene C. Butcher[1]

[1]Laboratory of Immunology and Vascular Biology, Department of Pathology, Stanford University School of Medicine, Stanford, CA 94305, and Center for Molecular Biology and Medicine, Veterans Affairs Palo Alto Health Care System, Palo Alto, CA 94304
[2]Department of Pathology, Stanford University School of Medicine, Stanford, CA 94305
[3]Inflammation Department, Millennium Pharmaceuticals, Cambridge, MA 02139
[4]Skaggs School of Pharmacy and Pharmaceutical Sciences, University of California, San Diego, La Jolla, CA 92093
[5]Department of Anatomy, Chonbuk National University Medical School, Jeonju, Republic of Korea
[6]Department of Microbiology and Immunology, Stanford University School of Medicine, Stanford, CA 94305

Mast cells contribute importantly to both protective and pathological IgE-dependent immune responses. We show that the mast cell–expressed orphan serpentine receptor mCCRL2 is not required for expression of IgE-mediated mast cell–dependent passive cutaneous anaphylaxis but can enhance the tissue swelling and leukocyte infiltrates associated with such reactions in mice. We further identify chemerin as a natural nonsignaling protein ligand for both human and mouse CCRL2. In contrast to other "silent" or professional chemokine interreceptors, chemerin binding does not trigger ligand internalization. Rather, CCRL2 is able to bind the chemoattractant and increase local concentrations of bioactive chemerin, thus providing a link between CCRL2 expression and inflammation via the cell-signaling chemerin receptor CMKLR1.

CORRESPONDENCE
Stephen J. Galli:
sgalli@stanford.edu
OR
Brian A. Zabel:
bazabel@alum.mit.edu

Abbreviations used: ANOVA, analysis of variance; BMCMCs, BM-derived cultured mast cells; CCRL2, chemokine (CC motif) receptor-like 2; CMKLR1, chemokine-like receptor 1; DNP-HSA, 2,4-DNP-conjugated human serum albumin; GPCR, G protein–coupled receptor; HA, hemagglutinin; PCA, passive cutaneous anaphylaxis.

Leukocyte-expressed orphan heptahelical receptors that share significant homology with known chemoattractant receptors, yet remain uncharacterized with respect to ligand binding properties and functions, represent excellent candidates for additional regulators of immune cell trafficking and function. Given its phylogenetic homology with members of the CC chemokine receptor subfamily, orphan serpentine receptor chemokine (CC motif) receptor-like 2 (CCRL2; also known as L-CCR [LPS-inducible C-C chemokine receptor related gene] or Eo1 in mice, and HCR [human chemokine receptor], CRAM-A, CRAM-B, or CKRX [chemokine receptor X] in humans) has been identified as a potential leukocyte chemoattractant receptor. However, CCRL2 possesses an uncharacteristic intracellular loop 2 sequence in place of the DRYLAIV motif generally found in signaling chemokine receptors (QRYLVFL in huCCRL2 and QRYRVSF in mCCRL2), leading us to postulate that it might be an "atypical" silent or nonsignaling receptor. From a phylogenetic standpoint, CCRL2 may be unique, as its orthologues are more divergent

B. Zabel and S. Nakae contributed equally to this paper.
S. Nakae's present address is National Research Institute for Child Health and Development, Tokyo, Japan.
J.-Y. Kim and J. Pan's present address is Bayer Healthcare Pharmaceuticals, Inc., Berkeley, CA.
T. Ohyama's present address is Daiichi Sankyo Co., Ltd., Tokyo, Japan.
C. Alt's present address is SRI International, Menlo Park, CA.
H. Suto's present address is Atopy Research Center, Juntendo University, Tokyo, Japan.
The online version of this article contains supplemental material.

The Rockefeller University Press $30.00
J. Exp. Med. Vol. 205 No. 10 2207-2220
www.jem.org/cgi/doi/10.1084/jem.20080300

The Journal of Experimental Medicine

in sequence that any other mouse-to-man receptor pair in the chemoattractant G protein–coupled receptor (GPCR) subfamily. The sequence identity of mouse and human CCRL2 is only 51%, compared with ~80% identity between most other receptor orthologues (1–3).

mCCRL2 was initially shown to be up-regulated at the RNA level in peritoneal macrophages treated with LPS (3). In experimental autoimmune encephalomyelitis, a murine model of multiple sclerosis, CCRL2 RNA is expressed in the spinal column early during the onset of disease by astrocytes, microglia, and infiltrating macrophages (4). Astrocytes and microglia also up-regulate mCCRL2 in response to LPS (5). In a model of ovalbumin-induced airway inflammation, infiltrating lung macrophages express CCRL2 RNA after ovalbumin challenge, whereas the bronchial epithelium is constitutively positive for expression (6). By mAb staining, huCCRL2 is expressed by circulating human T cells, neutrophils, monocytes, $CD34^+$ BM precursors, and monocyte-derived macrophages and DCs and is generally up-regulated upon activation of such cells (7). HuCCRL2 is also expressed on synovial fluid neutrophils (from rheumatoid arthritis patients) and is up-regulated on freshly isolated blood neutrophils treated with LPS or TNFα (8). Although there is a study indicating that CCR2 ligands such as CCL2 act as functional ligands for CCRL2 (9), this finding remains controversial (8; for review see reference 10).

Several atypical serpentine GPCRs that are homologous to chemoattractant receptors bind to chemoattractants but fail to transduce intracellular signals through heterotrimeric G proteins and/or support cell migration. This functionally defined receptor subfamily is currently thought to be comprised of three members: D6, DARC (Duffy antigen receptor for chemokines), and CCX-CKR (ChemoCentryx chemokine receptor) (for review see references 10, 11). These receptors are also referred to as professional chemokine "interceptors," a name which reflects their ability to efficiently internalize bound ligand (12). These receptors also lack the consensus DRYLAIV-related sequence present in the second intracellular loop domain of most chemokine receptors, possibly accounting for their inability to transduce classical intracellular signals (the sequence is DKYLEIV in D6, LGHRLGA in DARC, and DRYWAIT in CCX-CKR). Identifying ligands for "silent" or nonsignaling orphan receptors has proven to be particularly challenging because the assays employed in most GPCR ligand screens generally depend on functional responses, such as intracellular calcium mobilization, cell migration, or transcriptional activation.

D6 is expressed by lymphatic endothelium and by some leukocytes and binds proinflammatory CC chemokines. It is constitutively internalized (independent of chemokine binding) and can rapidly degrade large quantities of chemokines (13). DARC is expressed by vascular endothelium and is present on RBCs. It binds mostly proinflammatory chemokines (both CC and CXC types), and its expression on RBCs can buffer levels of circulating chemokines (14, 15). DARC-bound chemokines on erythrocytes are not presented or transferred to other chemokine receptors (16). Endothelial cell–expressed DARC may be able to transcytose certain chemokines, although this finding is controversial (17, 18). CCX-CKR mRNA is expressed in many tissues, including lymph node, spleen, placenta, kidney, brain, and by leukocytes. It binds the homeostatic chemokines CCL19, CCL21, and CXCL13 and has been shown to be able to degrade large quantities of CCL19 (19). Genetic deficiencies in D6 or DARC have been associated with exacerbated or dysregulated inflammatory responses, reflecting the importance of interceptors in dampening chemokine-mediated activities (for review see reference 10).

We and others identified chemerin as a natural nonchemokine chemoattractant ligand for chemokine-like receptor-1 (CMKLR1) (20–22). CMKLR1 is expressed by circulating human plasmacytoid DC (pDC) but not by circulating or tissue mouse DC (20, 23). In contrast, tissue resident macrophages in both humans and mice express CMKLR1 (23). A recent study by Parolini et al. (24) describes CMKLR1 expression by human NK cells. We and others have demonstrated that activation of chemerin involves proteolytic processing of the carboxyl terminus and removal of inhibitory amino acids (22, 25–27; for review see reference 28). Various serine proteases of the coagulation, fibrinolytic, and inflammatory cascades can activate chemerin, including plasmin, factor XII, and neutrophil elastase and cathepsin G (27). Mast cell tryptase, released upon antigen-mediated cross-linking of surface IgE/FcεRI on mast cells, is a particularly potent activator of chemerin (27). We have also demonstrated that chemerin circulates at low nanomolar concentrations in plasma in an immature inactive proform (for review see reference 28). We hypothesize that chemerin may serve as a nearly ubiquitous "humor" poised to translate tissue damage or bleeding into rapidly generated attractant fields for specialized CMKLR1-positive cells.

Mast cells, tissue-dwelling derivatives of circulating mast cell progenitors, are anatomically deployed to host-environment boundaries (such as the skin, airways, and alimentary canal) where they can mediate first-line encounters with pathogens and environmental allergens (29). Antigen-mediated cross-linking of surface IgE/FcεRI triggers mast cell degranulation and the release of preformed proinflammatory mediators stored in the cells' cytoplasmic granules, such as histamine, heparin, and proteases (e.g., tryptases, chymases, and cathepsins), and initiates the synthesis and release of lipid mediators (e.g., prostaglandin D_2 and leukotrienes) and diverse cytokines, chemokines, and growth factors (30). Localized IgE-mediated mast cell "anaphylactic-type" degranulation can be modeled in vivo by experimental IgE-dependent passive cutaneous anaphylaxis (PCA) in mice.

In this paper, we generated novel mAbs specific for the orphan GPCR mCCRL2 and demonstrated that freshly isolated mouse peritoneal mast cells selectively express the receptor. mCCRL2 KO mice displayed no overt phenotype and had normal numbers of mast cells in the tissues analyzed. When tested in vitro, BM-derived cultured mast cells (BMCMCs)

of mCCRL2 KO mouse origin exhibited responses to IgE and specific antigen-mediated cross-linking of FcεRI that were statistically indistinguishable from those of WT BMCMCs. In IgE-dependent PCA reactions in vivo, a model of IgE-mediated local anaphylaxis, mast cell–expressed CCRL2 was not required for the development of cutaneous inflammatory responses in mice sensitized with a high dose of antigen-specific IgE. However, mast cell–expressed CCRL2 was required for the development of optimal cutaneous tissue swelling and leukocyte infiltrates in mice sensitized with a low dose of antigen-specific IgE.

To investigate the mechanism by which CCRL2 may contribute to inflammation, we sought to identify potential CCRL2 ligands. In experiments based on binding rather than functional output, we identified chemerin as a novel non-signaling protein ligand for both human and mouse receptors. As opposed to chemokine interceptors that serve as a sink for chemokines upon their ligand-induced internalization, chemerin is not rapidly internalized by CCRL2. Rather, CCRL2 concentrates the chemoattractant and increases local chemerin concentrations available to interact with CMKLR1. We propose that CCRL2 is a novel attractant receptor, serving to focus chemerin localization in vivo and contribute to CMKLR1-mediated processes that, in turn, regulate pathways leading to increased vascular permeability, tissue swelling, and leukocyte recruitment.

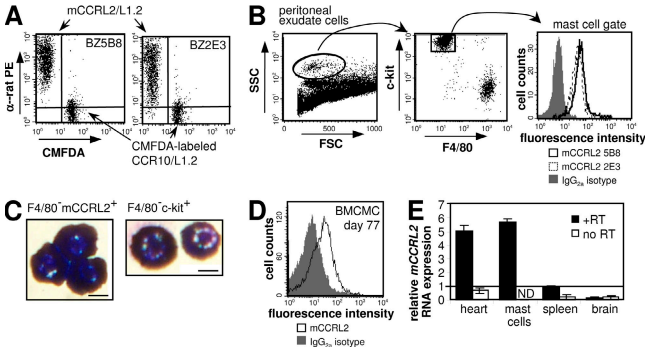

Figure 1. Mast cells express mCCRL2. (A) Generation of anti-mCCRL2 specific mAbs. Unlabeled mCCRL2/L1.2 transfectants were mixed 1:1 with CMFDA-labeled CCR10/L1.2 transfectants and used to identify mCCRL2-specific mAbs by flow cytometry. (B) Freshly isolated peritoneal leukocytes were harvested and mCCRL2 expression was evaluated on SSC^{high} $F4/80^{-}$ c-kit^{+} mast cells. (C) $F4/80^{-}$ mCCRL2^{+} and $F4/80^{-}$ c-kit^{+} peritoneal cells were sorted, harvested by cytospin, and stained by Wright-Giemsa. Cells were examined by light microscope using a 40× objective. Bars, 10 µm. (D) BMCMCs were generated and stained for mCCRL2 reactivity. (E) The relative RNA expression of mCCRL2 was assessed in mast cells by real-time quantitative PCR. The expression data were normalized to *Cyclophilin A* and displayed relative to *mCCRL2* expression in the spleen (set = 1). Each bar represents the mean ± SD of triplicate wells. ND, not detectable. One representative dataset of the at least three experiments, each of which gave similar results, is shown for each part of this figure.

RESULTS

mCCRL2-specific mAbs selectively stain mouse mast cells

We generated monoclonal antibodies BZ5B8 and BZ2E3 ($IgG_{2a}\kappa$) with reactivity to the extracellular amino-terminal domain of mCCRL2 (Fig. 1 A). The antibodies were specific to mCCRL2-hemagglutinin (HA)/L1.2 transfectants, displaying no cross-reactivity with other GPCR/L1.2 transfectants tested (mCMKLR1, huCMKLR1, mCRTH2, huCCRL2, or mCCR10). Reactivity with CXCR1–6 and CCR1–10 was excluded by lack of staining of blood cell subsets or cultured mouse cells known to express these receptors (Fig. S1, available at http://www.jem.org/cgi/content/full/jem.20080300/DC1; and not depicted). In agreement with published RNA expression data (3), peritoneal macrophages treated with LPS up-regulated mCCRL2 protein expression. Expression of mCCRL2 was also up-regulated in such cells by treatment with TNFα, IFN-γ, or poly:IC (Fig. S2 A).

Freshly isolated mouse blood T cells, B cells, NK cells, BM neutrophils, and resting peritoneal macrophages were all negative for mCCRL2 expression (Fig. S1 A). A small population of highly granular (SSC^{high}) $F4/80^{-}$ c-kit^{+} leukocytes in the peritoneal cavity, however, uniformly stained for mCCRL2 (Fig. 1 B). These cells also expressed the high-affinity IgE Fc receptor FcεRI (unpublished data). On staining with Wright-Giemsa stain, sorted $F4/80^{-}$CCRL2^{+} cells displayed intense metachromatic staining of abundant cytoplasmic granules, as did mast cells sorted as $F4/80^{-}$ c-kit^{+} cells (Fig. 1 C). Thus, both traditional morphological and immunophenotypic analyses indicate that mCCRL2 is constitutively expressed by mast cells, and the expression is surprisingly selective for mast cells in the absence of pathological stimuli.

Mast cells derived from BM progenitors in vitro (BMCMCs) up-regulated expression of mCCRL2 over time in culture. Early mast cell progenitors were negative for mCCRL2, but after >2 mo in culture, the cells uniformly expressed detectable levels of mCCRL2, albeit with lower levels than those on peritoneal mast cells in vivo (Fig. 1 D). We confirmed RNA expression of mCCRL2 in peritoneal mast cells by real-time quantitative RT-PCR (Fig. 1 E).

CCRL2 and mast cell phenotype and function

We evaluated numbers of mast cells in CCRL2 KO mice in vivo, as well as certain basic functions of CCRL2 KO BMCMC in vitro. Our anti-mCCRL2 mAbs failed to stain peritoneal mast cells from CCRL2 KO mice, confirming the genetic ablation of the gene (Fig. 2 A). The mice are fertile, reproduce with the expected Mendelian distribution of KO/heterozygotes/WT and male/female ratios, and display no differences in basal mast cell numbers in the ear skin or in mesenteric windows (Fig. 2 B).

CCRL2 KO and WT BMCMCs expressed similar levels of c-kit (CD117) and FcεRI (unpublished data). BMCMCs from WT or mCCRL2 KO mice also displayed similar chemotactic responses to stem cell factor (SCF), indicating no inherent differences in cell migration (Fig. 3 A), similar degranulation responses to antigen-mediated IgE/FcεRI cross-linking as assessed by β-hexosaminidase release (Fig. 3 B), and similar activation-dependent secretion of cytokines TNFα

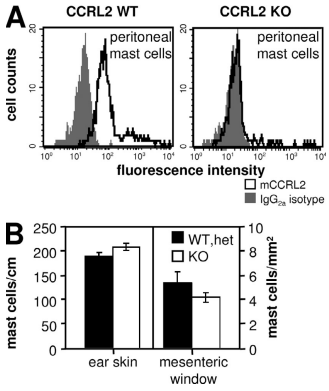

Figure 2. *mCCRL2* KO mice. (A) *mCCRL2* KO mice are deficient in CCRL2 protein expression. Freshly isolated peritoneal leukocytes were harvested and mCCRL2 expression was evaluated on $SSC^{high}F4/80^{-}$ $ckit^{+}$ mast cells. A representative histogram plot of the at least three independent experiments performed, each of which gave similar results, is shown. (B) Enumeration of ear skin and mesenteric mast cells in WT and KO mice. Ear skin: KO (n = 9), WT,het (n = 4,1), 4 sections/mouse. Mesenteric window: KO (n = 18), WT,het (n = 9,2). The mean ± SEM is displayed.

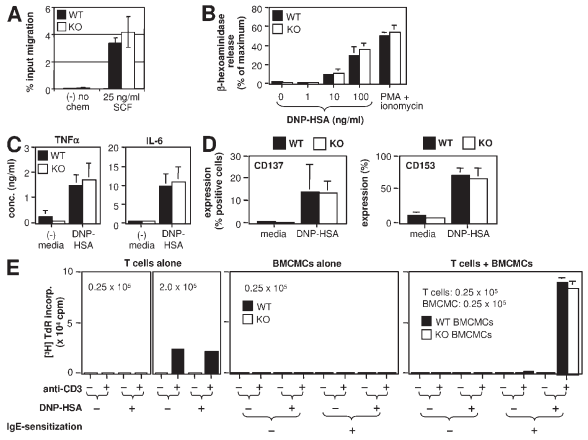

Figure 3. BMCMCs from *mCCRL2* KO and WT mice display similar functional responses in vitro. (A) In vitro transwell chemotaxis to SCF. Four populations of BMCMCs were tested, with duplicate wells for each genotype. The mean ± SEM is displayed. (B–D) BMCMCs were sensitized with DNP-specific IgE and then activated by addition of DNP-HSA. The following parameters were measured: Degranulation (as quantified by β-hexosaminidase release; B), TNFα and IL-6 secretion (C), and up-regulation of costimulatory molecules CD137 and CD153 (D). (E) BMCMC-stimulated T cell proliferation. Naive T cells were incubated as indicated with anti-CD3 and cocultured with mitomycin C–treated BMCMCs from WT or CCRL2 KO mice preincubated with or without DNP-specific IgE and tested in the presence or absence of DNP-HSA. Cell proliferation was measured by tritiated thymidine incorporation. For B, C, and D, n = 7 KO, n = 4 WT, mean ± SD. For E, the mean of triplicate measurements ± SD is shown for a representative dataset of three experiments (each of which gave similar results).

and IL-6 (Fig. 3 C). We recently showed that antigen-mediated IgE/FcεRI cross-linking up-regulated expression of several costimulatory molecules on BMCMCs (31); however, we did not detect any CCRL2-dependent differences in CD137 (4-1BB) or CD153 (CD30L) induction (Fig. 3 D). BMCMCs stimulated by antigen-mediated IgE/FcεRI cross-linking also can enhance T cell proliferation (31, 32). Although naive T cells proliferated markedly in response to treatment with anti-CD3 and coincubation with mitomycin C–treated antigen-specific IgE-stimulated BMCMCs, there were no CCRL2-dependent differences in the ability of BMCMCs to enhance T cell proliferation (Fig. 3 E) or T cell secretion of IFN-γ or IL-17 (not depicted) in the conditions tested. Thus, the presence of absence of CCRL2 on BMCMCs did not significantly influence the basic mast cell functions tested here.

Mast cell–expressed CCRL2 is required for optimal induction of IgE-dependent PCA

To search for potential contributions of CCRL2 to pathophysiologic responses in vivo, we next examined certain inflammatory conditions that are known to involve mast cells. Mast cells are required for optimal expression of the T cell–mediated contact hypersensitivity (CHS) induced by a protocol using FITC but not that induced by other protocols using DNFB (2,4-dinitro-1-fluorobenzene) (33, 34). However, CCRL2 was largely dispensable for the tissue swelling associated with FITC-triggered CHS, as both WT and CCRL2 KO mice developed statistically indistinguishable responses (Fig. S3, available at http://www.jem.org/cgi/content/full/jem.20080300/DC1).

We next examined a mast cell–dependent model of atopic allergy, the IgE-dependent PCA reaction. Animals sensitized with 150 ng/ear DNP-specific IgE and challenged with antigen (2,4-DNP-conjugated human serum albumin [DNP-HSA]) i.v. developed strong local inflammatory responses, with no significant difference in the tissue swelling observed in WT versus CCRL2 KO mice (82 ± 9 vs. $91 \pm 9 \times 10^{-2}$ mm of swelling at 30 min after antigen challenge, respectively; $P > 0.05$, Student's t test; Fig. S4 A, available at http://www.jem.org/cgi/content/full/jem.20080300/DC1). However, when the sensitizing dose of DNP-specific IgE was reduced to 50 ng/ear, the PCA reactions in CCRL2 KO mice were significantly impaired compared with those in WT mice (42.2 ± 2.8 vs. $24.9 \pm 2.7 \times 10^{-2}$ mm of swelling at 30 min after antigen challenge, respectively; $P < 0.005$, Student's t test; Fig. 4 A).

To assess the extent to which mCCRL2 expression specifically on mast cells was critical for the defect in IgE-dependent PCA observed in mCCRL2 KO mice, we engrafted mast cell–deficient $Kit^{W\text{-}sh/Wsh}$ mice intradermally in the ear pinnae with either WT or mCCRL2 KO BMCMCs. 6–8 wk later, the animals were subjected to IgE-dependent PCA. Such mast cell engraftment of mast cell–deficient $Kit^{W\text{-}sh/Wsh}$ or $Kit^{W/W\text{-}v}$ mice is routinely used to identify the roles of mast cells in biological responses in vivo (29). There was no difference in the extent of PCA-associated ear swelling between $Kit^{W\text{-}sh/Wsh}$ mice that had been engrafted with WT versus

mCCRL2 KO BMCMCs when the animals were sensitized with 50 ng/ear DNP-specific IgE and challenged with i.v. antigen (19.5 ± 3.6 vs. 19.9 ± 2.6 × 10^{-2} mm of swelling at 30 min after antigen challenge, respectively; $P > 0.05$, Student's *t* test; Fig. S4 B). Nor was there a significant difference in the numbers of leukocytes infiltrating the dermis at these sites at 6 h after antigen challenge (Figs. S4 C and S5).

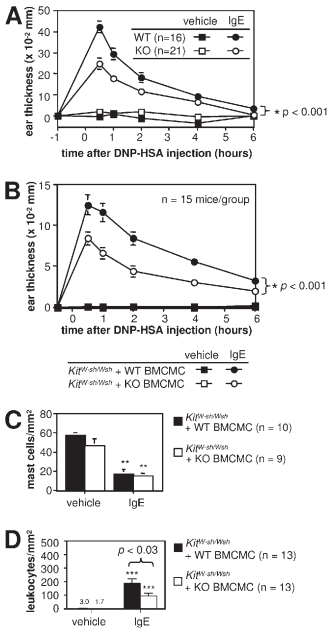

Figure 4. Mast cell–expressed mCCRL2 is required for maximal tissue swelling and numbers of dermal leukocytes in PCA. (A) WT or CCLR2 KO mice were sensitized by injection of 50 ng of anti-DNP IgE into left ear skin (with vehicle injection into right ear skin as the control). The mice were challenged by i.v. injection of DNP-HSA (200 µg/mouse) the next day, and ear swelling was measured at the indicated time points (mean ± SEM; $n = 3$ experiments with a total of 21 KO and 16 WT mice per group). *, $P < 0.005$ by ANOVA comparing swelling in WT vs. KO ears sensitized with antigen-specific IgE. (B–D) The ears of mast cell–deficient $Kit^{W\text{-}sh/Wsh}$ mice were engrafted with BMCMCs from either WT or mCCRL2 KO mice. 6–8 wk later, the mice were sensitized (5 ng IgE/left ear, with vehicle into the right ear as the control), challenged with specific antigen (200 µg DNP-HSA i.v.), and assessed for tissue swelling (B), as described in A, and for numbers of mast cells (C) or leukocytes (D) per millimeters squared of dermis. Data are shown as mean ± SEM, $n = 3$ experiments, with 15 total mice per group in B, and the numbers of mice sampled for histological data are shown in C and D. *, $P < 0.001$ by ANOVA comparing swelling in mCCRL2 KO BMCMC- vs. WT BMCMC-engrafted ears sensitized with antigen-specific IgE. (C) Enumeration of mast cells present in the dermis of ear skin in engrafted animals from B after elicitation of PCA (IgE) or in vehicle-injected control (vehicle) ears. **, $P < 0.005$ by Student's *t* test versus values for the vehicle-injected ears in the corresponding WT BMCMC- or KO BMCMC-engrafted $Kit^{W\text{-}sh/Wsh}$ mice. (D) Numbers of leukocytes per millimeters squared of dermis, assessed in formalin-fixed paraffin-embedded hematoxylin and eosin–stained sections of mice from B and C. ***, $P < 0.0001$ by the Mann Whitney *U* test versus corresponding values for the vehicle-injected ears in WT BMCMC- or KO BMCMC-engrafted $Kit^{W\text{-}sh/Wsh}$ mice. The numbers over the bars for vehicle-injected mice are the mean values.

However, when the sensitizing dose of DNP-specific IgE was reduced to 5 ng/ear, there was a significant reduction in ear swelling responses in mice that had been engrafted with mCCRL2 KO BMCMCs compared with those that had been engrafted with WT BMCMCs (12.5 ± 1.2 vs. 8.4 ± 0.8 × 10^{-2} mm of swelling at 30 min after antigen challenge, respectively; $P < 0.01$, Student's *t* test; Fig. 4 B). There were no significant differences in the total number of mast cells detected histologically in WT versus CCRL2 KO BMCMC-engrafted ears, thus ruling out any CCRL2-dependent effects on mast cell engraftment efficiency (Fig. 4 C). However, at 6 h after antigen challenge, IgE-dependent PCA reactions in ears that had been engrafted with CCRL2 KO mast cells contained ~50% fewer leukocytes (predominantly neutrophils and mononuclear cells) than did reactions in ears that had been engrafted with WT mast cells ($P < 0.03$, Mann Whitney *U* test; Fig. 4 D and Fig. 5). IgE-dependent PCA reactions were associated with a marked reduction in the numbers of dermal mast cells that could be identified in histological sections of these sites based on the staining of the cells' cytoplasmic granules (Fig. 4 C), an effect which most likely reflected extensive mast cell degranulation at these sites (35, 36).

We conclude that although mast cell–expressed mCCRL2 is not required for the development of IgE-dependent PCA reactions in vivo, mast cell expression of CCRL2 can significantly enhance the local tissue swelling and leukocyte infiltrates associated with such reactions in mice that have been sensitized with relatively low amounts of antigen-specific IgE.

CCRL2 binds chemerin

To investigate possible functional roles for CCRL2, we set out to validate/identify CCRL2 ligands. It was reported that

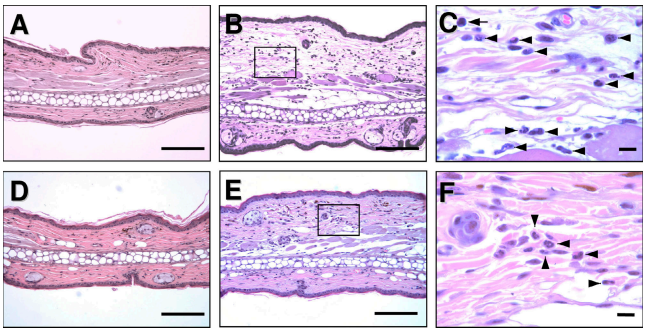

Figure 5. Histological features of IgE-dependent PCA reactions in WT BMCMC- versus KO BMCMC-engrafted $Kit^{W\text{-}sh/Wsh}$ mice. Histological sections of ear skin from WT BMCMC-engrafted $Kit^{W\text{-}sh/Wsh}$ mice (A–C) and KO BMCMC-engrafted $Kit^{W\text{-}sh/Wsh}$ mice (D–F) from the same group shown in Fig. 4 D analyzed 6 h after i.v. injection of DNP-HSA show no evidence of inflammation in vehicle-sensitized ears (A and D), but evidence of tissue swelling and increased numbers of leukocytes in DNP-specific IgE-sensitized ears (B, C, E, and F). Enlargements of the boxed regions in B and E are shown in C and F, respectively. The inflammatory infiltrate consists predominantly of polymorphonuclear leukocytes (some indicated by arrowheads in C and F) and occasional mononuclear cells (indicated by an arrow in C). Bars, 50 µm.

mCCRL2/HEK293 transfectants respond functionally to CCR2 ligands CCL2, CCL5, CCL7, and CCL8 via intracellular calcium mobilization and transwell chemotaxis (9), although this conclusion is controversial (8; for review see reference 10). These chemokines did not induce migration of mCCRL2/L1.2 transfectants in our in vitro transwell chemotaxis assays (Fig. S6, available at http://www.jem.org/cgi/content/full/jem.20080300/DC1). We also tested a panel of known chemoattractants (CCL11, CCL17, CCL22, CCL25, CCL27, CCL28, CXCL9, and CXCL13), as well as protein extracts from homogenized mouse tissues (lungs, kidney, liver, brain, and spleen), and found that none stimulated mCCRL2-dependent chemotaxis in our in vitro transwell chemotaxis assays (unpublished data). Given the aberrant DRYLAIV motif that is present in mouse and human CCRL2, we and others postulated that mCCRL2 may act as a silent receptor (for review see reference 10), which is capable of binding chemoattractants but incapable of transducing signals via classical second messengers. That hypothesis is consistent with the negative results obtained in our efforts to induce chemotaxis of mCCRL2/L1.2 transfectants in our in vitro transwell chemotaxis assays.

Although we failed to identify evidence of signaling effects of any of the tested chemoattractants, we were able to identify a high-affinity ligand for the receptor: in independent studies in which we were using our anti-CCRL2 mAbs as controls for staining, we serendipitously discovered that chemerin, a protein ligand for signaling receptor CMKLR1 (for review see reference 28), inhibited the binding of mCCRL2-specific mAbs to mouse peritoneal mast cells. In Fig. 6 A, we illustrate the potent ability of chemerin to inhibit anti-CCRL2 staining of mouse peritoneal mast cells. Increasing concentrations of chemerin blocked the binding of anti-mCCRL2 BZ5B8 (Fig. 6 A) and BZ2E3 (not depicted) in a dose-dependent manner (EC_{50} = 21 nM). The effect was specific to anti-mCCRL2:mCCRL2 interactions because binding of IgE to FcRεI was unaffected by 1,000 nM chemerin (Fig. 6 A), and 1,000 nM CCL2 had no effect on CCRL2 staining (Fig. 6 A).

To confirm the identification of CCRL2 as a chemerin receptor, we performed radioligand binding studies using iodinated chemerin. Cells were incubated with a fixed concentration of radiolabeled human chemerin plus increasing concentrations of unlabeled chemerin. Chemerin bound specifically to mCCRL2-HA/L1.2 transfectants (EC_{50} = 1.6 nM; Fig. 6 B), but no binding was detected to untransfected or mCRTH2-HA–transfected cells (a prostaglandin D_2 binding chemoattractant receptor; not depicted). Furthermore, despite being the most divergent mouse-to-man orthologues in the chemoattractant receptor subfamily, huCCRL2 also bound specifically to chemerin (EC_{50} = 0.2 nM; Fig. 6 B). The binding affinity of chemerin for CCRL2 was similar to, if not slightly better than, chemerin binding to the first identified chemerin receptor, mCMKLR1 (EC_{50} = 3.1 nM; Fig. 6 B). In saturation binding studies, chemerin bound to mCCRL2 at a single binding site with a calculated kD of 1.6 nM (Fig. 6 C).

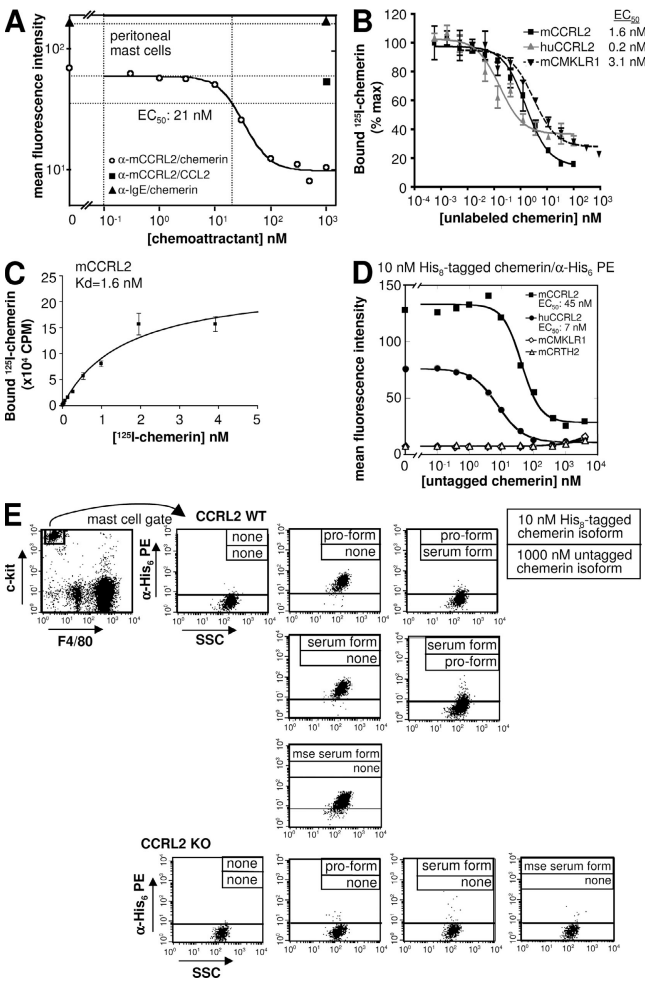

Figure 6. CCRL2 binds chemerin. (A) Chemerin blocks anti-CCRL2 mAb binding. Various concentrations of human chemerin or CCL2 were incubated with total peritoneal mast cells on ice for 5 min, followed by incubation with CCRL2-specific mAb BZ2E3 or anti-IgE and detected with secondary anti-rat PE or anti-mouse IgE PE. (B and C) Radiolabeled chemerin binding. (B) Displacement of iodinated chemerin (residues 21–148) binding to mCMKLR1, huCCRL2, and mCCRL2 by full-length chemerin. (C) Saturation binding of ^{125}I-chemerin$_{21-148}$ to mCCRL2-transfected cells. (D) Immunofluorescence-based chemerin binding. Various concentrations of untagged serum form chemerin were incubated with mCCRL2-HA, huCCRL2-HA, mCRTH2-HA, or mCMKLR1-HA L1.2 transfectants in the presence of 10 nM His_8-tagged serum form chemerin. Samples were incubated on ice for 30 min. Secondary anti-His_6 PE was added to detect levels of bound His_8-tagged chemerin, and mean fluorescence intensity values are displayed. Mean fluorescence intensity ± range of duplicate staining wells are shown. (E) Mast cell binding. 1,000 nM of untagged chemerin isoforms were incubated with total peritoneal cells from either WT or CCRL2 KO mice in the presence or absence of 10 nM His_8-tagged chemerin isoforms. Secondary anti-His_6 PE was added to detect levels of bound His_8-tagged chemerin. SSC^{high} $F4/80^{-}$ c-kit^{+} mast cells were analyzed. For B and C, the mean of quadruplicate wells ±SD is shown for individual experiments. A representative dataset of the three (for B, D, and E) or two experiments (for A and C) performed, each of which gave similar results, is shown.

We developed an immunofluorescence-based chemerin-binding assay to evaluate chemerin binding by flow cytometry. Cells were incubated with a fixed concentration of C-terminal His_8-tagged serum form human chemerin plus increasing concentrations of untagged chemerin, and anti-His_6 PE was used to detect binding. In this assay, chemerin bound specifically to mCCRL2-HA (EC_{50} = 45 nM) and huCCRL2 (EC_{50} = 7 nM) L1.2 transfectants (Fig. 6 D). Chemerin binding to CCRL2 was not affected by a variety of other chemoattractants (Fig. S7, available at http://www.jem.org/cgi/content/full/jem.20080300/DC1), and mCRTH2-HA/L1.2 transfectants did not bind to chemerin (Fig. 6 D), demonstrating specificity for chemerin–CCRL2 interactions. Interestingly, we were unable to detect chemerin binding to mCMKLR1-HA/L1.2 transfectants in the immunofluorescence chemerin binding assay (Fig. 6 D). This may reflect inhibition of binding by the C-terminal His_8 tag (which would be analogous to the inhibitory activity of the carboxyl-terminal residues in the chemerin proform) or, potentially, inaccessibility of the His_8 epitope to the detection mAbs when His_8-tagged chemerin is bound to CMKLR1.

In radioligand binding studies, the His_8 tag had little effect on the potency of chemerin binding to mCCRL2 (EC_{50} = 0.8 nM); however, His_8-tagged chemerin bound with 10-fold less potency to mCMKLR1 (EC_{50} = 26.3 nM; Fig. S8 A, available at http://www.jem.org/cgi/content/full/jem.20080300/DC1). The bioactive 9-mer carboxyl-terminal chemerin peptide (residues 149–157, YFPGQFAFS) was 10-fold less potent (EC_{50} = 26.2 nM; see Fig. 8 A) than chemerin protein in binding to CMKLR1. In CCRL2 binding, however, the bioactive chemerin peptide was an inefficient competitor (EC_{50} could not be determined, Fig. S8 B). Thus, the data indicate distinct binding modes for chemerin and CCRL2 versus chemerin and CMKLR1. The carboxyl-terminal domain of chemerin that is critical for binding to CMKLR1 is relatively uninvolved and unencumbered when chemerin is bound to CCRL2.

Freshly isolated mouse peritoneal mast cells also bound to chemerin (Fig. 6 E), and there was no obvious preference for binding of the proform versus the active serum form (this was also observed in radioligand binding studies using L1.2 transfectants; not depicted). Moreover, mouse peritoneal mast cells bound both human and mouse chemerin (Fig. 6 E). Finally, peritoneal mast cells from mCCRL2 KO mice did not bind to chemerin, further confirming the role of CCRL2 in the binding of chemerin to such mast cells (Fig. 6 E).

CCRL2 does not support chemerin-driven signal transduction

Despite high-affinity binding to mCCRL2, chemerin failed to trigger intracellular calcium mobilization in mCCRL2/L1.2 transfectants (Fig. 7 A). Chemerin triggered a robust calcium flux in cells expressing the chemerin signaling receptor mCMKLR1, confirming its activity (Fig. 7 A). mCCRL2-HA/L1.2 transfectants responded to CXCL12 (via endogenous CXCR4), indicating their competence for demonstrating calcium mobilization in this assay (Fig. 7 A). Furthermore, although it was reported that CCL2 triggered intracellular calcium mobilization in CCRL2/HEK293 transfectants, in our experiments neither CCL2 nor chemerin functioned as agonists for CCRL2 in the HEK293 background, either alone or in combination (Fig. S9, available at http://www.jem.org/cgi/content/full/jem.20080300/DC1).

Because GPCR function can require cell type–specific cofactors, we wanted to determine whether CCRL2 could mediate chemerin signaling when expressed physiologically on mouse peritoneal mast cells. Chemerin did not trigger intracellular calcium mobilization in freshly isolated mouse peritoneal mast cells, although these cells responded to ATP (via purinoreceptors [reference 37]), indicating their competence in this assay (Fig. 7 B). Furthermore, neither human nor mouse CCRL2-HA/L1.2 transfectants migrated to a range of doses of chemerin in in vitro transwell chemotaxis experiments (Fig. 7 C). Freshly isolated mouse peritoneal mast cells also failed to migrate to chemerin (Fig. 7 D). In comparison, chemerin triggered a robust dose-dependent migratory response in mCMKLR1-HA/L1.2 cells (Fig. 7 C). Mouse and human CCRL2/L1.2 cells migrated to CXCL12 and CCL19 (via endogenously expressed CXCR4 and CCR7, respectively),

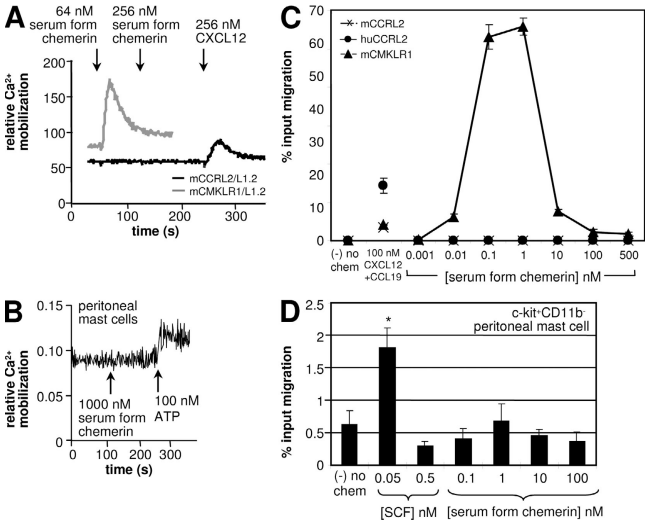

Figure 7. Chemerin–CCRL2 binding does not trigger intracellular calcium mobilization or chemotaxis. (A) mCCRL2 and mCMKLR1 L1.2 transfectants were loaded with Fluo-4, treated with chemerin and/or CXCL12 at the indicated times, and examined for intracellular calcium mobilization. (B) Mouse peritoneal mast cells were enriched by NycoPrep density centrifugation, loaded with Fura-2 and Fluo-4, and assayed for calcium mobilization. 1,000 nM chemerin and 100 nM ATP were added as indicated. (C) mCCRL2-HA, huCCRL2-HA, and mCMKLR1-HA L1.2 transfectants were tested for transwell chemotaxis to various concentrations of chemerin. The mean ± range of duplicate wells is shown. (D) Mouse peritoneal mast cells were assayed for in vitro chemotaxis to various concentrations of SCF and chemerin. Mast cells were identified by gating on SSC^{high} $CD11b^-$ $c\text{-}kit^+$ cells. The mean ± SD of triplicate wells is shown for an individual experiment. *, $P < 0.01$ by Student's *t*-test comparing migration to 0.05 nM SCF versus (−) no chem. A representative dataset of the three experiments performed, each of which gave similar results, is shown for all parts of this figure.

and primary mouse peritoneal mast cells migrated to stem cell factor (SCF), indicating their ability to demonstrate chemotaxis is this assay (Fig. 7, C and D). Furthermore, CCL2 and chemerin did not synergize with each other to induce a functional migratory response in mCCRL2/L1.2 transfectants in in vitro transwell migration assays (unpublished data).

CCRL2 does not internalize chemerin

Our data place CCRL2 in a class of atypical receptors that include D6, DARC, and CCX-CKR, all of which bind to chemoattractants but do not support classical ligand-driven signal transduction (for review see reference 11). These other receptors have recently been termed professional "chemokine interceptors" because they internalize and either degrade and/or transcytose chemokines (for review see [10,11]) (12). To ask whether CCRL2 might have interceptor activity, we assessed the internalization of CCRL2, and of CMKLR1 for comparison, in response to ligand binding. mCMKLR1-HA internalized rapidly (within 15 min) in response to 100 nM chemerin, and this internalization was inhibited by incubation on ice and in the presence of sodium azide (Fig. 8 A), confirming that the effect is an active process (not caused by chemerin-mediated displacement of the anti-HA mAb). In contrast, under the same conditions, CCRL2 failed to internalize. Neither mouse nor human CCRL2, expressed on L1.2 transfectants, underwent ligand-induced internalization (Fig. 8 A). Even prolonged incubation with chemerin (2 h at 37°C) failed to significantly reduce surface receptor levels (unpublished data).

We also asked whether CCRL2 might undergo constitutive ligand-independent endocytosis, as has been observed with D6 (13). Cell surface mCCRL2-HA and mCMKLR1-HA were stained with primary anti-HA mAb on ice, washed, and then shifted to 37°C for various times to permit receptor internalization. The cells were then stained with a secondary antibody to detect remaining surface anti-HA mAb. At the 15-min time point, neither mCCRL2 nor mCMKLR1 had undergone substantial ligand-independent endocytosis, which is similar to CCX-CKR (19) and in contrast to D6 (13). By 60 min there was a noticeable reduction in staining intensity for both human and mouse receptors, suggesting low-level constitutive endocytosis, receptor turnover, and/or antibody release (Fig. 8 B).

Given that chemerin does not trigger mCCRL2 internalization, it is unlikely that chemerin itself is internalized in substantial amounts in CCRL2$^+$ cells (in the absence of CMKLR1). To confirm this directly, we loaded mCCRL2-HA/L1.2 cells with His_8-tagged serum form chemerin and anti-His_6 PE on ice and then shifted the cells to 37°C to permit internalization. At the indicated time points, the cells were washed with either PBS or a high-salt acid wash buffer that strips bound chemerin from the surface of the cell (Fig. 8 C, zero time point). In contrast to D6 and CCX-CKR, where >70% of cell-associated CCL3 (13) and 100% of cell-associated CCL19 (19) became resistant to acid wash within 5 min, respectively, there was essentially no acid-resistant

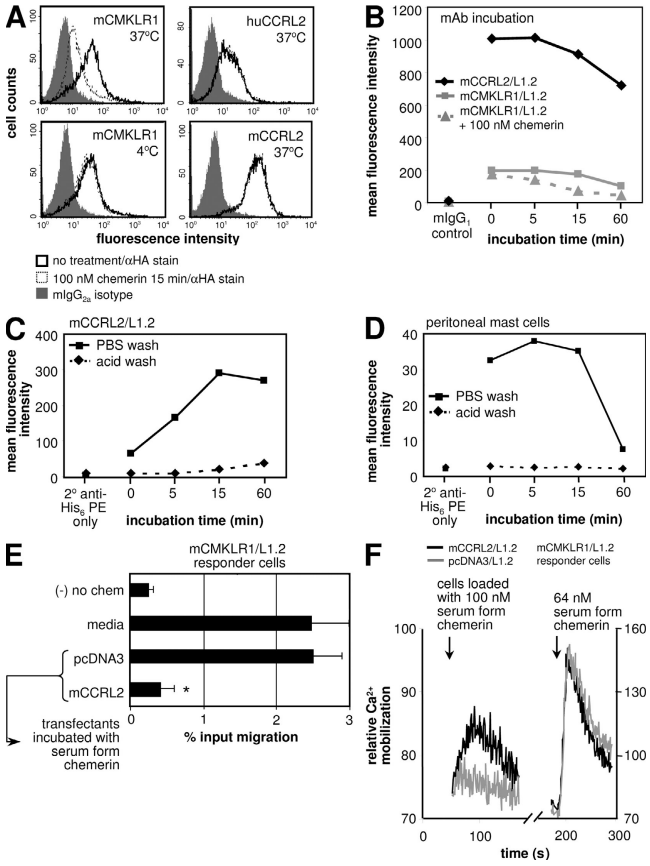

Figure 8. CCRL2 can increase local chemerin concentrations. (A) Chemerin does not trigger CCRL2 receptor internalization. mCCRL2-HA, huCCRL2-HA, and mCMKLR1-HA L1.2 transfectants were stained with anti-HA mAb and then incubated with or without 100 nM chemerin for 15 min at the indicated temperatures. (B) mCCRL2 is not rapidly constitutively internalized. mCCRL2-HA and mCMKLR1-HA L1.2 transfectants were incubated with primary anti-HA mAb, incubated for the indicated times at 37°C, and then stained with secondary anti-mIgG1 PE. mCMKLR1 cells incubated with 100 nM of serum-form chemerin served as a positive control. (C and D) Chemerin is not rapidly internalized. mCCRL2-HA L1.2 transfectants (C) or total peritoneal exudate cells (D) were incubated with 10 nM His_8-tagged serum form chemerin and anti-His_6 PE for 1 h on ice and then shifted to 37°C. At the indicated time points, the cells were then washed with either PBS or acid wash buffer. Mast cells were identified by gating on SSC^{high} F4/80$^-$ c-kit$^+$ cells in D. (E) CCRL2 can sequester chemerin from solution. 2 nM of serum-form chemerin was incubated with the indicated transfectant lines (or media alone) for 15 min at 37°C. The cells were removed by centrifugation, and the conditioned media was tested in transwell chemotaxis using mCMKLR1HA/L1.2 responder cells. The mean ± SD of triplicate wells for an individual experiment is shown. (F) CCRL2 can increase local concentrations of bioactive chemerin. mCCRL2-HA or empty vector pcDNA3 L1.2 transfectants were preloaded with 1,000 nM of serum-form chemerin and washed with PBS. mCMKLR1/L1.2 loaded with Fluo-4 served as responder cells. The intracellular calcium mobilization in the responder cells was measured over time as loaded cells or purified chemoattractant was added. Note that different scales are used on either side of the broken-axis indicator. A representative dataset of the three experiments performed, each of which gave similar results, is shown for all parts of this figure.

cell-associated chemerin at the 5-min time point and very little at the 60-min time point (Fig. 8 C). In contrast, there was a time-dependent increase in surface-bound chemerin (Fig. 8 C, PBS wash). Freshly isolated peritoneal mouse mast cells also did not internalize chemerin (Fig. 8 D, acid wash). In contrast to mCCRL2/L1.2 transfectants, however, at the 60-min time point there was a considerable reduction in surface-bound chemerin (Fig. 8 D, PBS wash), suggesting either eventual extracellular degradation or chemerin release. Furthermore, mCCRL2-HA/L1.2 transfectants efficiently bound chemerin from dilute aqueous solutions (Fig. 8 E). Thus, it appears that CCRL2 binds and indeed concentrates chemerin on the cell surface.

Finally, we wanted to assess whether chemerin sequestered by mCCRL2$^+$ cells could trigger a response in mCMKLR1$^+$ cells. We loaded empty vector pcDNA3 or mCCRL2-HA L1.2 cells with chemerin, washed with PBS, added the loaded cells to mCMKLR1/L1.2 responder cells labeled with a calcium-sensitive dye, and assessed intracellular calcium mobilization. Chemerin-loaded mCCRL2-HA/L1.2 cells, but not pcDNA3/L1.2 cells, triggered calcium flux in the responder cells (Fig. 8 F). Thus, CCRL2 can concentrate bioactive chemerin, which then is available for interaction with CMKLR1 on adjacent cells.

DISCUSSION

The evolutionary conservation of chemerin binding to CCRL2 despite divergence in overall sequence between mouse and human receptors strongly suggests that the interaction of chemerin with CCRL2 is physiologically important. The lack of substantial chemerin internalization by CCRL2 disqualifies the receptor as a professional chemoattractant interceptor and, instead, implicates it as a physiological mediator for the concentration and presentation of bioactive chemerin. We hypothesize, therefore, that CCRL2 serves a novel role among cell surface chemoattractant receptors, regulating the bioavailability of chemerin in vivo to fine-tune immune responses mediated via the signaling receptor CMKLR1. Chemerin inhibits the binding of mAbs specific to amino-terminal epitopes of mCCRL2, implying that chemerin binds directly to the amino-terminal domain of the receptor. In this regard, it is interesting to note that the first 16 aa of human and mouse CCRL2 share 81% identity, compared with just 17% shared identity in the remaining 24 aa of the amino-terminal domain (Fig. S10, available at http://www.jem.org/cgi/content/full/jem.20080300/DC1). This short conserved amino-terminal sequence may therefore embody a critical chemerin binding domain. Furthermore, CCRL2 binds to chemerin in an orientation that permits antibody access to the short C-terminal His_8 tag, suggesting that the critical cell-signaling carboxyl terminus of chemerin would also be exposed in the untagged form of the protein. Thus, we hypothesize that CCRL2 (e.g. expressed by mast cells and activated macrophages) binds to chemerin in vivo and presents the cell-signaling carboxyl-terminal domain of the chemoattractant to CMKLR1$^+$ cells such as macrophages, pDC, and NK cells (Fig. 9). In its role as a specialized molecule for concentrating extracellular chemerin, CCRL2 may operate akin to glycosaminoglycans, which are thought to bind, concentrate, and present chemokines to leukocytes and facilitate their chemotaxis (38).

In experimental IgE-dependent PCA, a simple in vivo model of an IgE- and mast cell–dependent acute allergic reaction, CCLR2-deficient mice expressed WT levels of tissue swelling when the mice were sensitized with one dose of antigen-specific IgE but exhibited significantly reduced tissue swelling associated with PCA reactions elicited in mice sensitized with one third less antigen-specific IgE. This clearly shows that mast cell expression of CCLR2 is not required for elicitation of IgE-dependent PCA but may substantially enhance reactions elicited under conditions where IgE may be limiting. PCA has been widely used to study factors involved in mast cell responses in vivo (39, 40). In our previous studies, we showed that pro-chemerin is rapidly activated by extracellular serine proteases such as secreted mast cell tryptase (27). Thus, the acute nature of the PCA reaction is well suited to highlight possible consequences of rapid chemerin conversion in vivo. CCRL2 expression by tissue mast cells may serve to coat the cells with the proform of chemerin, which would be immediately activated upon mast cell degranulation and tryptase release (27).

The reason why the tissue swelling associated with IgE-dependent PCA reactions in CCRL2 KO mice was less than that observed in WT mice is not yet clear. The largest differences in the tissue swelling responses of the WT versus KO mice (or in the mast cell–deficient mice that had been

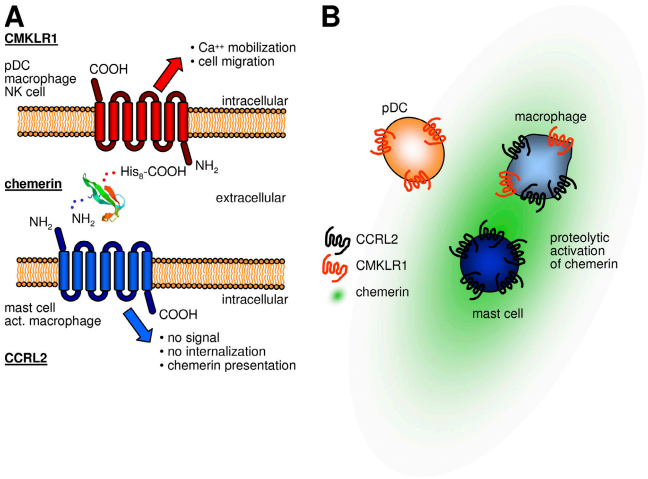

Figure 9. Proposed model of presentation of chemerin by CCRL2 to CMKLR1. (A) Chemerin binds to CCRL2 leaving the C-terminal peptide sequence free. The carboxyl-terminal domain of chemerin is critical for transducing intracellular signals and interacts directly with CMKLR1. CCRL2 may thus allow direct presentation of bound chemerin to adjacent CMKLR1-expressing cells. (B) Alternatively, CCRL2 may concentrate the ligand for proteolytic processing by activated mast cells or macrophages, enhancing the local production of the active form which could then act as a chemoattractant after release from the cell surface.

engrafted with WT vs. KO BMCMCs) were at 30 min after i.v. antigen challenge, an interval which is too short to observe substantial recruitment of circulating leukocytes to the site of the reaction. Perhaps mast cell–bound and then activated chemerin interacts with $CMKLR1^+$ macrophages or other mononuclear cells that might be present in normal skin, and such cells in turn have effects that can enhance local vascular permeability. Alternatively, other cell types normally resident in the skin, such as vascular endothelial cells, may respond to locally activated chemerin. The reduced leukocyte numbers present in the dermis 6 h after the elicitation of IgE-dependent PCA reactions in mice whose dermal mast cells lacked CCLR2 indicates that a lack of mast cell CCLR2 also can diminish the longer term consequences of IgE-dependent cutaneous reactions, perhaps by multiple mechanisms (which are yet to be defined). Mast cells themselves are $CMKLR1^-$ (Fig. S11). Notably, the inflammation associated with relatively strong PCA reactions was not substantially affected by the presence of absence of CCRL2, whether on all cells types (Fig. S4A) or only on skin mast cells (Fig. S4, B and C). Thus, whatever contribution mast cell–associated CCRL2 makes to the tissue swelling and leukocyte infiltrates associated with PCA responses appears to enhance tissue sensitivity to suboptimal IgE-dependent mast cell activation.

Treatment of peritoneal macrophages with proinflammatory cytokines (IFN-γ and TNFα) or TLR ligands (LPS and poly:IC but not CpG) up-regulates CCRL2 expression (Fig. S2 A) (3). We observed synergistic effects on receptor up-regulation when TNFα or IFN-γ treatment was combined with LPS. An analysis of transcription factor binding sites revealed an interferon-stimulated response element (ISRE) upstream of the CCRL2 promoter, which is conserved among mammals and may be responsible for the IFN-γ–mediated regulation of gene expression in macrophages (Fig. S2 B). LPS and IFN-γ did not influence CCRL2 expression on similarly treated peritoneal mast cells (unpublished data). The constitutive expression of CCRL2 on freshly isolated mast cells and the regulated expression of CCRL2 on macrophages indicates that there can be cell type–specific regulation of CCRL2 gene expression. Furthermore, it is interesting to note that CCRL2 and CMKLR1 on macrophages are reciprocally regulated (e.g., LPS causes down-regulation of CMKLR1 but up-regulation of CCRL2 (Fig. S2 A) (23). Our data indicate that at some point before 24 h after activation by TLR ligands or proinflammatory cytokines, macrophages can concurrently express both chemerin receptors CMKLR1 and CCRL2. The functional consequence of this is under investigation.

CCRL2 may play distinct physiological roles depending on the cellular context of its expression. In a general survey of mouse tissues, mCCRL2 is expressed at the RNA level in the lung, heart, and spleen, with minimal expression in the brain or thymus (Fig. S12, available at http://www.jem.org/cgi/content/full/jem.20080300/DC1). CCRL2 expression by stromal cells in the lung and heart may serve to maintain a reservoir of chemerin and to buffer tissue levels of the attractant in vivo in the same manner that erythrocyte-expressed atypical chemokine receptor DARC can serve as a buffer to maintain chemokine levels in the blood (14, 15). We are currently investigating this hypothesis by comparing chemerin protein levels in blood and tissue extracts from WT and CCRL2 KO mice.

Transfectant-expressed CCRL2 has been reported to bind CCL2 and CCL5, although this result is controversial (9). CCL2 did not interfere with anti-mCCRL2 mAb staining in our studies. In addition, using either the binding conditions published in this paper for chemerin or those published by Biber et al. (9) for CCL2, we were unable to confirm the binding of biotinylated CCL2 to CCRL2/L1.2 transfectants (unpublished data). However, it is unclear whether the biotinylated CCL2 reagent available to us is useful for identifying cognate receptor expression because we observed similar high background binding of this reagent to T cells in WT and CCR2 KO mice.

The identification of natural ligands for silent or nonsignaling receptors (such as D6, DARC, and CCX-CKR) has lagged behind the deorphaning of signaling receptors. This is likely because of an intrinsic bias toward GPCR-ligand screening methods that rely on measuring functional responses (e.g., calcium mobilization or chemotaxis), rather than binding, per se, to identify "hits". Although there are >100 orphan heptahelical GPCR sequences that have been identified via genome sequencing (41), the phylogenetic homology of CCRL2 with CC chemokine receptors, and its expression at the RNA level by LPS activated macrophages, suggested that CCRL2 may be a modulator of leukocyte trafficking. Indeed, we show herein that the expression of CCLR2 by mast cells can enhance the numbers of leukocytes in the dermis at sites of IgE-dependent cutaneous inflammation (Fig. 4 D). The identification of chemerin as a nonsignaling ligand for CCRL2 introduces a novel functionality for atypical receptors (i.e., concentration and presentation, as we have shown herein for CCRL2, as opposed to internalization/degradation). Our findings expand the possible ligand space for atypical orphan receptors to include chemoattractants beyond the chemokine family and provide a potential link between CCRL2 expression and chemerin-dependent effects on inflammation that are mediated via the cell-signaling chemerin receptor CMKLR1.

MATERIALS AND METHODS

Antibodies and reagents. Anti-mouse CD11b, CD14, CD19, B220, Gr1, and TCRβ dye-linked mAb were obtained from eBioscience. Anti-mouse CD11c, c-kit, CD49b, and TER119 dye-linked mAb were obtained from BD Biosciences. Anti-mouse F4/80 FITC was obtained from AbD Serotec. Anti-rat phycoerythrin (human and mouse adsorbed) was purchased from BD Biosciences, anti-His_6 phycoerythrin was purchased from R&D Systems, purified Fc block (mouse anti–mouse CD16.2/32.2) was purchased from Invitrogen, anti-mCMKLR1 (BZ194) was prepared in house, and mouse IgG, rat IgG, and goat serum were purchased from Sigma-Aldrich. CCL2-5,7-9,11,16,17,19-22,25,28; CXCL1,2,3,9,10,12,13,16; IL-4; GM-CSF; and Flt-3 ligand were purchased from R&D Systems. Mouse CCL2

biotinylated fluorokine kit was purchased from R&D Systems. CMFDA, Fluo-4-acetoxymethyl (AM), and Pluronic acid F-127 (reconstituted in DMSO) were purchased from Invitrogen. Bioactive chemerin peptide (YFPGQFAFS) was synthesized by the Stanford PAN facility. Phosphothioated CpG oligonucleotides (42) were purchased from QIAGEN. polyI:C and FMLP were purchased from Sigma-Aldrich. LPS (*Escherichia coli* O11:B4-derived) was purchased from List Biological Laboratories, Inc. TNFα and IFN-γ were purchased from Roche. CFA and IFA were purchased from Sigma-Aldrich. Cytokine levels in culture supernatants were measured by using mouse TNFα and IL-6 BD OptEIA ELISA Sets (BD Biosciences).

Animals. The Veterans Affairs Palo Alto Health Care System Institutional Animal Care and Use Committee (Palo Alto, CA) and the Stanford University Administrative Panel on Laboratory Animal Care (Stanford, CA) approved all animal experiments. CCRL2 KO mice (Lexicon) were backcrossed four generations on the C57BL/6 background. Mast cell deficient $Kit^{W\text{-}sh/Wsh}$ mice on the C57BL/6 background (43) were provided by P. Besmer (Memorial Sloan-Kettering Cancer Center and Cornell University Graduate School of Medical Sciences, NY, NY), and WT C57BL/6 mice were obtained from Taconic. Wistar Furth rats were obtained from Charles River Laboratories.

Mammalian expression vector construction and generation of stable cell lines. The coding regions of mCCRL2, huCCRL2, mCRTH2, and huCCR10 were amplified from genomic DNA with or without an engineered N-terminal HA tag and cloned into pcDNA3 (Invitrogen). Transfectants were generated and stable lines selected in the mouse pre–B lymphoma cell line L1.2 or HEK293 cells as previously described (44). mCMKLR1 and empty vector L1.2 transfectants were generated as previously described (20). Transfected cells were, in some cases, treated with 5 mM *n*-butyric acid (Sigma-Aldrich) for 24 h before experimentation (45).

Generating the anti-mCCRL2 mAbs BZ5B8 and BZ2E3. The immunizing amino-terminal mCCRL2 peptide with the sequence NH_2-MDNYTVAPDDEYDVLILDDYLDNSC-COOH (corresponding to residues 1–24 of mCCRL2, with a nonnative carboxyl-terminal cysteine to facilitate conjugation to keyhole limpet hemocyanin [KLH]) was synthesized by the Stanford Protein and Nucleic Acid Biotechnology Facility and conjugated to KLH according to the manufacturer's specifications (Thermo Fisher Scientific). Wistar Furth rats were immunized with the mCCRL2 peptide/KLH conjugate, first emulsified in CFA and then, subsequently, in IFA. Hybridomas producing anti-mCCRL2 mAbs were subcloned, and specificity was confirmed by reactivity with mCCRL2 but not other L1.2 receptor transfectants. An ELISA-based assay (BD Biosciences) was used to assess the $IgG_{2a}κ$ isotypes of the resulting rat anti–mouse CCRL2 mAbs, designated BZ5B8 and BZ2E3.

Harvesting mouse leukocytes. Mice were given a fatal overdose of anesthesia (ketamine/xylazine), as well as an i.p. injection of 100 U heparin (Sigma-Aldrich), and blood was collected by cardiac puncture. Up to 1 ml of blood was added to 5 ml of 2 mM EDTA in PBS, and 6 ml of 2% dextran T500 (GE Healthcare) was added to cross-link RBCs. The mixture was incubated for 1 h at 37°C, the supernatant was removed and pelleted, and the cells were resuspended in 5 ml of RBC lysis buffer (Sigma-Aldrich) and incubated at room temperature for 5 min. The cells were pelleted and resuspended for use in cell staining. BM cells were harvested by flushing femurs and tibias with media followed by RBC lysis. Peritoneal lavage cells were obtained by i.p. injection of 10 ml PBS, gentle massage of the peritoneal cavity, and collection of the exudate. For some experiments, 500 µl of peritoneal cells (2×10^6 cells/ml) were incubated for 24 h with 1 µg/ml LPS, 10 ng/ml TNFα, 100 U/ml IFN-γ, 20 µg/ml polyI:C, 10–100 µg/ml CpG, or 5 ng/ml TGFβ. For mast cell RNA isolation, peritoneal mast cells were enriched for by density centrifugation. Approximately 140 million peritoneal exudate cells were harvested from nine male WT mice >1 yr of age. The cells were resuspended in 10 ml PBS and underlaid with 5 ml NycoPrep 1.077A (Axis-Shield). After centrifugation, ∼140,000 high-density mast cells were recovered at the bottom of the tube (along with ∼100,000 contaminating RBCs). For functional assays using primary mast cells, peritoneal lavage was performed using Tyrode's solution, and the cells were kept at room temperature throughout harvest.

Cell sorting and Wright-Giemsa stain. Mouse peritoneal cells were stained as described and sorted by standard flow cytometric techniques (FACSVantage; BD Biosciences; flow cytometry was performed at the Stanford University Digestive Disease Center Core Facility, VA Hospital, Palo Alto, CA). $1–5 \times 10^4$ sorted cells were loaded into cytospin chambers and centrifuged onto glass slides. The slides were stained with Wright-Giemsa dye by standard automated techniques at the VA Hospital Hematology Laboratory (Palo Alto, CA) and examined by light microscopy with a 40× objective (CX-2; Olympus).

RNA expression analysis. RNA from the indicated tissues or cells was extracted using an RNeasy kit per the supplier's instructions (QIAGEN). Gene expression was determined by quantitative PCR using a real-time PCR instrument (7900HT; Applied Biosystems) equipped with a 384-well reaction block. 0.3–1.0 µg of total RNA was used as a template for cDNA synthesis using MMLV Reverse transcription (Applied Biosystems) with oligo dT primers, according to the supplier's instructions. The cDNA was diluted and amplified by quantitative PCR in triplicate wells using 10 pmols of gene specific primers in a total volume of 10 µl with Power SYBR Green qPCR Master Mix (Applied Biosystems), according to manufacturer's instructions. CCRL2 gene expression was normalized to *cyclophilin A* (*cycA*) levels in each tissue and displayed relative to CCRL2 expression levels detected in the spleen using the $2^{-\Delta\Delta CT}$ method (46). Primers used were the following: m*CCRL2* 5′, ttccaacatcctcctccttg; m*CCRL2* 3′, gatgcacgcaacaataccac; *cycA* 5′, gagctgtttgcagaccaaagttc; and *cycA* 3′, ccctggcacatgaatcctgg. An RNA dot blot array was purchased from BD Biosciences, and hybridizations were performed according to the manufacturer's recommendation. A full-length gel-purified mCCRL2 cDNA probe was radiolabeled with ^{32}P using Rediprime reagents (GE Healthcare) according to the manufacturer's specifications.

Preparation of BMCMCs. Mouse femoral BM cells were cultured in 20% WEHI-3 cell conditioned medium (containing IL-3) for 6–12 wk, at which time the cells were >98% c-kit^{high} FcεRIα^{high} by flow cytometry analysis.

β-hexosaminidase release assay. BMCMCs were sensitized with 10 µg/ml of anti-DNP IgE mAb (H1-ε-26; reference 47) by overnight incubation at 37°C. The cells were then washed with Tyrode's buffer (10 mM Hepes, pH 7.4, 130 mM NaCl, 5 mM KCl, 1.4 mM $CaCl_2$, 1 mM $MgCl_2$, 0.1% glucose, and 0.1% BSA [fraction V; Sigma Aldrich]) and resuspended at 8×10^6 cells/ml. 25 µl of a 2× concentration of stimuli (final: 0, 1, 10, and 100 ng/ml DNP-HSA [Sigma-Aldrich] or 0.1 µg/ml PMA [Sigma-Aldrich] + 1 µg/ml A23187 calcium ionophore [Sigma-Aldrich]) were added to the wells of a 96-well V-bottom plate (Costar; Corning), and then 25 µl of 8×10^6 cells/ml IgE-sensitized BMCMCs were added and incubated at 37°C for 1 h. After centrifugation, supernatants were collected. The supernatants from nonstimulated IgE-sensitized BMCMCs treated with 50 µl of 0.5% (vol/vol) Triton X-100 (Sigma-Aldrich) were used to determine the maximal (100%) cellular β-hexosaminidase content, to which the experimental samples were normalized. β-hexosaminidase release was determined by enzyme immunoassay with *p*-nitrophenyl-*N*-acetyl-β-D-glucosamine (Sigma-Aldrich) substrate as follows: 10 µl of culture supernatant was added to the wells of a 96-well flat-bottom plate. 50 µl of 1.3 mg/ml *p*-nitrophenyl-*N*-acetyl-β-D-glucosamine solution in 100 mM sodium citrate, pH 4.5, was added, and the plate was incubated at room temperature for 15–30 min. Next, 140 µl of 200 mM glycine, pH 7, was added to stop the reaction, and the OD_{405} was determined.

T cell–mast cell coculture. For $CD3^+$ T cell purification, a single cell suspension of spleen cells was prepared, and RBCs were lysed (RBC lysing buffer). Spleen cells were incubated with biotinylated anti–mouse B220, Gr-1, CD11b, CD11c, CD49b, Ter119, and c-kit for 20 min at 4°C. The cells were then washed and incubated with streptavidin-beads (Miltenyi Biotec) for 20 min at 4°C, washed again, and passed through a magnetic cell-sorting column (MACS column; Miltenyi Biotec), yielding >95% $CD3^+$ T cells. T cells were cocultured with mast cells as described previously (32). BMCMCs were sensitized with 1 μg/ml of anti-DNP IgE mAb at 37°C overnight. After IgE sensitization, BMCMCs were treated with mitomycin C (50 μg/10^7 cells; Sigma-Aldrich) for 15 min at 37°C. BMCMCs and T cells were suspended in RPMI 1640 media (Cellgro; Mediatech, Inc.) supplemented with 50 μM 2-mercaptoethanol (Sigma-Aldrich), 50 μg/ml streptomycin (Invitrogen), 50 U/ml penicillin (Invitrogen), and 10% heat inactivated FCS (Sigma-Aldrich). 0.25×10^5 T cells/well were plated in a 96-well flat-bottom plate (BD Biosciences) coated with 1 μg/ml anti–mouse CD3 (clone 145-2C11; BD Biosciences) or hamster IgG (eBioscience; in some experiments, anti-CD3 (−) indicates the substitution of control IgG for anti-CD3), and mitomycin C-treated IgE-sensitized or nonsensitized BMCMCs (0.25×10^5 cells/well) in the presence or absence of 5 ng/ml DNP-HSA at 37°C for 72 h. Proliferation was assessed by pulsing with 0.25 μCi ^{3}H-thymidine (GE Healthcare) for 6 h, harvesting the cells using Harvester 96 Mach IIIM (Tomtec, Inc.) and measuring incorporated ^{3}H-thymidine using a Micro Beta System (GE Healthcare).

PCA reaction. Experimental PCA was performed as previously described (48), with minor modifications. Mice were injected intradermally with 20 μl of either anti-DNP IgE mAb (H1-ε-26; 5, 50, or 150 ng) in the left ear skin or vehicle alone (Pipes-HMEM buffer) in the right ear skin. The next day, mice received 200 μl of 1 mg/ml DNP-HSA (200 μg/mouse) i.v. Ear thickness was measured before and at multiple intervals after DNP-HSA injection with an engineer's microcaliper (Ozaki). For BMCMC engraftment experiments, BMCMCs were generated from either WT or LCCR KO mice, and 10^6 cells in 40 μl DMEM were injected into the ear skin of mast cell–deficient $Kit^{W\text{-}sh/Wsh}$ mice. 6–8 wk later, the mice were subjected to experimental PCA. After the assay, the mast cells in the ear skin were enumerated in formalin-fixed paraffin-embedded toluidine blue–stained sections to evaluate the extent of engraftment. In some experiments, formalin-fixed paraffin-embedded hematoxylin and eosin–stained sections were examined to enumerate numbers of leukocytes present in the dermis. In all histological studies, examination of the slides was performed by an observer who was not aware of the identity of individual sections.

FITC-induced contact hypersensitivity (CHS). FITC-induced CHS was performed as described previously (34) with minor modifications. Mice were shaved on abdomen 2 d before FITC sensitization. Mice were then treated with 200 μl of 2.0% (wt/vol) FITC isomer I (Sigma-Aldrich) suspension in acetone-dibutyl phthalate (1:1). 5 d after sensitization with 2.0% FITC, mice were challenged with 40 μl of vehicle alone to the right ear (20 μl to each side) and 0.5% (wt/vol) FITC solution to the left ear (20 μl to each side). Each mouse was housed in a separate cage to prevent contact with each other after FITC challenge. Ear thickness was measured before and at multiple intervals after FITC challenge with an engineer's microcaliper (Ozaki).

Chemerin expression and purification using baculovirus. The following carboxyl-terminal His_8-tagged proteins were expressed using baculovirus-infected insect cells as previously described (27): "serum form" human chemerin (NH_2-ADPELTE…FAPHHHHHHHH-COOH), "proform" human chemerin (NH_2-ADPELTE…LPRSPHHHHHH-COOH), and serum form mouse chemerin (NH_2-ADPTEPE…FAPHHHHHHHH-COOH). Because certain experiments required nontagged proteins, the His_8 tag was proteolytically removed by treatment with carboxypeptidase A (Sigma-Aldrich), generating the respective proteins NH_2-ADPELTE…FAPH-COOH, NH_2-ADPELTE…RSPH-COOH, and NH_2-ADPTEPE…FAPH-COOH, where the underlined residues are nonnative. The proteins were lyophilized and checked for purity using electrospray mass spectrometry.

Chemerin binding assays. For chemerin binding/anti-mCCRL2 mAbs displacement assays, total peritoneal exudate cells were incubated with various concentrations of chemerin or CCL2 for 5 min on ice in binding buffer, washed with PBS, and stained with primary antibodies (either anti-mCCRL BZ2E3 or IgE, + Fc block) for 45 min on ice. The cells were washed in PBS and stained with secondary anti-rat IgG PE or anti-mouse IgE PE (+ goat IgG) for 30 min on ice, washed with PBS, stained with directly conjugated F4/80 and c-kit mAbs, and analyzed by flow cytometry. For radioligand binding assays, radioiodinated chemerin (residues 21–148; R&D Systems; custom radiolabeling performed by PerkinElmer) was provided as a gift from J. Jaen (ChemoCentryx, Mountain View, CA). The specific activity of the ^{125}I-labeled chemerin was 97 Ci/g. For competition binding assays, L1.2 cells transfected with huCCRL2, mCCRL2, or mCMKLR1 were plated into 96-well plates at 0.5×10^6 cells/well. Cells were incubated in binding buffer (Hanks + 0.5% BSA) for 3 h at 4°C shaking with 1 nM ^{125}I-chemerin and increasing concentrations of chemerin, His_8-tagged chemerin, or peptide (9-aa YFPGQFAFS, corresponding to chemerin residues 149–157) as competitors. For saturation binding assays, mCCRL2/L1.2 cells were plated at 0.5×10^6 cells/well. Nonspecific binding was measured in the presence of 100 nM cold chemerin. Binding was terminated by washing the cells in saline buffer, and bound radioactivity was measured. Data were analyzed using Prism (GraphPad Software, Inc.). Binding data (triplicate or quadruplicate wells) were fitted to one-site binding hyperbola for saturation assays or to a one-site competition curve for competition assays. For direct chemerin binding immunofluorescence assays, mCCRL2-HA, huCCRL2-HA, mCMKLR1-HA, and mCRTH2-HA L1.2 transfectants were incubated for 30 min on ice with 10 nM His_8-tagged serum form human chemerin and the indicated concentration of untagged chemerin in binding buffer (PBS with 0.5% BSA and 0.02% azide). The cells were then washed with PBS and incubated with anti-His_6 PE (+ 2% goat serum) for 30 min on ice, washed, and analyzed by flow cytometry. Similar binding experiments were performed on total WT or CCRL2 KO peritoneal exudate cells with the indicated combinations and concentrations of proform or serum form His_8-tagged or untagged chemerin. After chemerin binding, the cells were stained with directly conjugated F4/80 and c-kit mAbs and analyzed by flow cytometry.

In vitro transwell chemotaxis. For migration experiments using cell lines, 2.5×10^5 cells/100 μl chemotaxis media (RPMI + 10% FCS) were added to the top wells of 5-μm pore transwell inserts (Costar; Corning), and test samples in 600 μl media were added to the bottom wells. After incubating the transwell plates for 1.5 h at 37°C, the bottom wells were harvested and flow cytometry was used to assess migration. For primary cell chemotaxis, 10^6 cells/100 μl were added to the top well and, after a 2-h incubation at 37°C, polystyrene beads (15.0 μm diameter; Polysciences, Inc.) were added to each well to facilitate normalization of the cell count. The cells were then stained for c-kit, F4/80, and/or CD11b expression and analyzed by flow cytometry. A ratio was generated and percent input migration was calculated.

Intracellular calcium mobilization. Chemoattractant-stimulated Ca^{2+} mobilization was performed according to Alliance for Cell Signaling protocol ID PP00000210. Cells (3×10^6/ml) were loaded with 4 μM Fluo4-AM and 0.16% Pluronic acid F-127 (Invitrogen) in modified Iscove's medium (Iscove's medium with 1% heat-inactivated bovine calf serum and 2 mM L-glutamine; Invitrogen) for 30 min at 37°C. The samples were mixed every 10 min during loading, washed once, resuspended at up to 2×10^6/ml in the same buffer, and allowed to rest in the dark for 30 min at room temperature. Chemoattractant-stimulated change in Ca^{2+}-sensitive fluorescence of Fluo-4 was measured over real-time with a FACScan flow cytometer and CellQuest software (BD Biosciences) at room temperature under constant stirring at 500 rpm. Fluorescent data were acquired continuously up to 1,024 s at 1-s intervals. The samples were analyzed for 45 s to establish basal state, removed

from the nozzle to add the stimuli, and then returned to the nozzle. Mean channel fluorescence over time was analyzed with FlowJo software (Tree Star, Inc.). In some experiments, to identify mast cells, mixed peritoneal leukocytes were preincubated with c-kit-PerCP mAb for 3 min immediately before the start of each sample. In other experiments, mCCRL2HA/L1.2 or empty vector pcDNA3/L1.2 cells were loaded for 30 min with 1,000 nM of serum form chemerin (incubated in binding buffer on ice), washed two times with PBS, and resuspended in Iscove's media at 2×10^6/ml. 500 µl of these chemerin-loaded cells were added to mCMKLR1/L1.2 cells loaded with Fluo4-AM, and calcium mobilization was evaluated.

Receptor internalization assay. mCMKLR1-HA, huCCRL2-HA, and mCCRL2-HA L1.2 transfectants were incubated for 15 min with 100 nM serum form chemerin at the indicated temperature in cell culture media. The cells were then washed with 200 µl PBS and stained with mouse anti-HA (Covance) or mIgG1 isotype control, followed by staining with secondary anti–mouse IgG1 PE, fixed, and analyzed by flow cytometry.

Ligand-independent receptor internalization assay. mCMKLR1-HA and mCCRL2-HA L1.2 transfectants were loaded for 30 min on ice with primary antibody (anti-HA or mIgG1 isotype control). The cells were washed with 200 µl PBS, incubated for the indicated times at 37°C to allow for receptor internalization, and then placed on ice. The cells were then incubated with secondary anti–mouse IgG_1 PE, and analyzed by flow cytometry.

Chemerin internalization assay. mCCRL2-HA L1.2 transfectants or total peritoneal exudate cells were incubated with 10 nM His_8-tagged serum form chemerin for 30 min on ice. The primary cells were also stained with F4/80 and c-kit mAbs. Secondary anti-His_6 PE was added to the cells and incubated for 30 min on ice. The cells were then incubated for the indicated times at 37°C to allow for chemerin internalization. The cells were incubated for 5 min on ice with either PBS or acid wash buffer (0.2 M acetic acid and 0.5 M NaCl) and then analyzed by flow cytometry. Mast cells were identified by gating on $SSC^{high}F4/80^{-}c\text{-}kit^{+}$ cells.

Chemerin sequestration assay. 2 nM of serum form chemerin was incubated with 40 million cells of the indicated transfectant lines (or media alone) for 15 min at 37°C. The cells were removed by centrifugation, and a volume of the conditioned media equivalent to 0.2 nM chemerin (barring any sequestration or degradation) was tested in transwell chemotaxis using mCMKLR1-HA/L1.2 cells.

Statistics. The unpaired Student's *t* test (two-tailed), Mann Whitney *U* test (two-tailed), or analysis of variance (ANOVA) was used for statistical evaluation of the results, as indicated.

Online supplemental material. Fig. S1 shows that blood lymphocytes, BM neutrophils, and peritoneal macrophages are negative for mCCRL2 expression. Fig. S2 shows that mCCRL2 is up-regulated on macrophages activated by specific cytokines and/or TLR ligands. Fig. S3 shows that mCCRL2 KO mice display a normal contact hypersensitivity response to FITC. Figs. S4 and S5 (histology of skin) show that mCCRL2 is dispensable for maximal tissue swelling and leukocyte infiltration in the dermis in high dose IgE-mediated PCA. Fig. S6 shows that mCCRL2/L1.2 transfectants do not migrate to CCL2, CCL5, CCL7, or CCL8 in in vitro transwell chemotaxis. Fig. S7 shows the lack of heterologous displacement of chemerin by other chemoattractants. Fig. S8 shows the displacement of iodinated chemerin (residues 21–148) binding to CCRL2 and CMKLR1 by His_8-chemerin and bioactive chemerin peptide (YFPGQFAFS). Fig. S9 shows the lack of intracellular calcium mobilization by CCL2 and/or chemerin in CCRL2/HEK293 transfectants. Fig. S10 shows an alignment of human and mouse CCRL2 amino-terminal sequences. Fig. S11 shows the lack of mCMKLR1 expression on peritoneal mast cells. Fig. S12 shows the mRNA expression profile of mCCRL2 using a RNA dot blot. Online supplemental material is available at http://www.jem.org/cgi/content/full/jem.20080300/DC1.

We thank Mindy Tsai, Kareem Graham, and J. Zabel for helpful discussions. We thank Dan Dairaghi, Tim Sullivan, Niky Zhao, and Susanna Lewén for assistance with the radioligand binding assays.

E.C. Butcher, B.A. Zabel, T. Ohyama, and J. Pan are supported by grants from the National Institutes of Health (AI-59635, AI-47822, and GM-37734), Specialized Center of Research (HL-67674), and Digestive Disease Center (DK-56339) and a Merit Award from the Veterans Administration to E.C. Butcher. S.J. Galli, S. Nakae, and H. Suto are supported by grants from the National Institutes of Health (HL-67674, AI-23990, AI-070813, and CA-72074). T.M. Handel is supported by grants from the National Institutes of Health (AI37113-09) and the California HIV/AIDS Research Program (ID06-SD-206). L. Zuniga is support by a National Institutes of Health pre-doctoral fellowship (AI073198). J.-Y. Kim was supported by the Serono Foundation and the Cancer Research Institute. C. Alt was supported by the Deutsche Forschungsgemeinschaft. S.J. Allen is supported by a California HIV/AIDS Research Program fellowship award (TF06-SD-501).

The authors have no conflicting financial interests.

Submitted: 13 February 2008
Accepted: 21 August 2008

REFERENCES

1. Fan, P., H. Kyaw, K. Su, Z. Zeng, M. Augustus, K.C. Carter, and Y. Li. 1998. Cloning and characterization of a novel human chemokine receptor. *Biochem. Biophys. Res. Commun.* 243:264–268.
2. DeVries, M.E., A.A. Kelvin, L. Xu, L. Ran, J. Robinson, and D.J. Kelvin. 2006. Defining the origins and evolution of the chemokine/chemokine receptor system. *J. Immunol.* 176:401–415.
3. Shimada, T., M. Matsumoto, Y. Tatsumi, A. Kanamaru, and S. Akira. 1998. A novel lipopolysaccharide inducible C-C chemokine receptor related gene in murine macrophages. *FEBS Lett.* 425:490–494.
4. Brouwer, N., M.W. Zuurman, T. Wei, R.M. Ransohoff, H.W. Boddeke, and K. Biber. 2004. Induction of glial L-CCR mRNA expression in spinal cord and brain in experimental autoimmune encephalomyelitis. *Glia.* 46:84–94.
5. Zuurman, M.W., J. Heeroma, N. Brouwer, H.W. Boddeke, and K. Biber. 2003. LPS-induced expression of a novel chemokine receptor (L-CCR) in mouse glial cells in vitro and in vivo. *Glia.* 41:327–336.
6. Oostendorp, J., M.N. Hylkema, M. Luinge, M. Geerlings, H. Meurs, W. Timens, J. Zaagsma, D.S. Postma, H.W. Boddeke, and K. Biber. 2004. Localization and enhanced mRNA expression of the orphan chemokine receptor L-CCR in the lung in a murine model of ovalbumin-induced airway inflammation. *J. Histochem. Cytochem.* 52:401–410.
7. Migeotte, I., J.D. Franssen, S. Goriely, F. Willems, and M. Parmentier. 2002. Distribution and regulation of expression of the putative human chemokine receptor HCR in leukocyte populations. *Eur. J. Immunol.* 32:494–501.
8. Galligan, C.L., W. Matsuyama, A. Matsukawa, H. Mizuta, D.R. Hodge, O.M. Howard, and T. Yoshimura. 2004. Up-regulated expression and activation of the orphan chemokine receptor, CCRL2, in rheumatoid arthritis. *Arthritis Rheum.* 50:1806–1814.
9. Biber, K., M.W. Zuurman, H. Homan, and H.W. Boddeke. 2003. Expression of L-CCR in HEK 293 cells reveals functional responses to CCL2, CCL5, CCL7, and CCL8. *J. Leukoc. Biol.* 74:243–251.
10. Mantovani, A., R. Bonecchi, and M. Locati. 2006. Tuning inflammation and immunity by chemokine sequestration: decoys and more. *Nat. Rev. Immunol.* 6:907–918.
11. Comerford, I., W. Litchfield, Y. Harata-Lee, R.J. Nibbs, and S.R. McColl. 2007. Regulation of chemotactic networks by 'atypical' receptors. *Bioessays.* 29:237–247.
12. Haraldsen, G., and A. Rot. 2006. Coy decoy with a new ploy: interceptor controls the levels of homeostatic chemokines. *Eur. J. Immunol.* 36:1659–1661.
13. Weber, M., E. Blair, C.V. Simpson, M. O'Hara, P.E. Blackburn, A. Rot, G.J. Graham, and R.J. Nibbs. 2004. The chemokine receptor D6 constitutively traffics to and from the cell surface to internalize and degrade chemokines. *Mol. Biol. Cell.* 15:2492–2508.
14. Hadley, T.J., and S.C. Peiper. 1997. From malaria to chemokine receptor: the emerging physiologic role of the Duffy blood group antigen. *Blood.* 89:3077–3091.

15. Darbonne, W.C., G.C. Rice, M.A. Mohler, T. Apple, C.A. Hebert, A.J. Valente, and J.B. Baker. 1991. Red blood cells are a sink for interleukin 8, a leukocyte chemotaxin. *J. Clin. Invest.* 88:1362–1369.
16. Kashiwazaki, M., T. Tanaka, H. Kanda, Y. Ebisuno, D. Izawa, N. Fukuma, N. Akimitsu, K. Sekimizu, M. Monden, and M. Miyasaka. 2003. A high endothelial venule-expressing promiscuous chemokine receptor DARC can bind inflammatory, but not lymphoid, chemokines and is dispensable for lymphocyte homing under physiological conditions. *Int. Immunol.* 15:1219–1227.
17. Middleton, J., S. Neil, J. Wintle, I. Clark-Lewis, H. Moore, C. Lam, M. Auer, E. Hub, and A. Rot. 1997. Transcytosis and surface presentation of IL-8 by venular endothelial cells. *Cell.* 91:385–395.
18. Lee, J.S., C.W. Frevert, M.M. Wurfel, S.C. Peiper, V.A. Wong, K.K. Ballman, J.T. Ruzinski, J.S. Rhim, T.R. Martin, and R.B. Goodman. 2003. Duffy antigen facilitates movement of chemokine across the endothelium in vitro and promotes neutrophil transmigration in vitro and in vivo. *J. Immunol.* 170:5244–5251.
19. Comerford, I., S. Milasta, V. Morrow, G. Milligan, and R. Nibbs. 2006. The chemokine receptor CCX-CKR mediates effective scavenging of CCL19 in vitro. *Eur. J. Immunol.* 36:1904–1916.
20. Zabel, B.A., A.M. Silverio, and E.C. Butcher. 2005. Chemokine-like receptor 1 expression and chemerin-directed chemotaxis distinguish plasmacytoid from myeloid dendritic cells in human blood. *J. Immunol.* 174:244–251.
21. Meder, W., M. Wendland, A. Busmann, C. Kutzleb, N. Spodsberg, H. John, R. Richter, D. Schleuder, M. Meyer, and W.G. Forssmann. 2003. Characterization of human circulating TIG2 as a ligand for the orphan receptor ChemR23. *FEBS Lett.* 555:495–499.
22. Wittamer, V., J.D. Franssen, M. Vulcano, J.F. Mirjolet, E. Le Poul, I. Migeotte, S. Brezillon, R. Tyldesley, C. Blanpain, M. Detheux, et al. 2003. Specific recruitment of antigen-presenting cells by chemerin, a novel processed ligand from human inflammatory fluids. *J. Exp. Med.* 198:977–985.
23. Zabel, B.A., T. Ohyama, L. Zuniga, J.Y. Kim, B. Johnston, S.J. Allen, D.G. Guido, T.M. Handel, and E.C. Butcher. 2006. Chemokine-like receptor 1 expression by macrophages in vivo: Regulation by TGF-beta and TLR ligands. *Exp. Hematol.* 34:1106–1114.
24. Parolini, S., A. Santoro, E. Marcenaro, W. Luini, L. Massardi, F. Facchetti, D. Communi, M. Parmentier, A. Majorana, M. Sironi, et al. 2007. The role of chemerin in the colocalization of NK and dendritic cell subsets into inflamed tissues. *Blood.* 109:3625–3632.
25. Wittamer, V., B. Bondue, A. Guillabert, G. Vassart, M. Parmentier, and D. Communi. 2005. Neutrophil-mediated maturation of chemerin: a link between innate and adaptive immunity. *J. Immunol.* 175:487–493.
26. Busmann, A., M. Walden, M. Wendland, C. Kutzleb, W.G. Forssmann, and H. John. 2004. A three-step purification strategy for isolation of hamster TIG2 from CHO cells: characterization of two processed endogenous forms. *J. Chromatogr. B Analyt. Technol. Biomed. Life Sci.* 811:217–223.
27. Zabel, B.A., S.J. Allen, P. Kulig, J.A. Allen, J. Cichy, T.M. Handel, and E.C. Butcher. 2005. Chemerin activation by serine proteases of the coagulation, fibrinolytic, and inflammatory cascades. *J. Biol. Chem.* 280:34661–34666.
28. Zabel, B.A., L. Zuniga, T. Ohyama, S.J. Allen, J. Cichy, T.M. Handel, and E.C. Butcher. 2006. Chemoattractants, extracellular proteases, and the integrated host defense response. *Exp. Hematol.* 34:1021–1032.
29. Galli, S.J., S. Nakae, and M. Tsai. 2005. Mast cells in the development of adaptive immune responses. *Nat. Immunol.* 6:135–142.
30. Kraft, S., S. Rana, M.H. Jouvin, and J.P. Kinet. 2004. The role of the FcepsilonRI beta-chain in allergic diseases. *Int. Arch. Allergy Immunol.* 135:62–72.
31. Nakae, S., H. Suto, M. Iikura, M. Kakurai, J.D. Sedgwick, M. Tsai, and S.J. Galli. 2006. Mast cells enhance T cell activation: importance of mast cell costimulatory molecules and secreted TNF. *J. Immunol.* 176:2238–2248.
32. Nakae, S., H. Suto, M. Kakurai, J.D. Sedgwick, M. Tsai, and S.J. Galli. 2005. Mast cells enhance T cell activation: Importance of mast cell-derived TNF. *Proc. Natl. Acad. Sci. USA.* 102:6467–6472.
33. Takeshita, K., T. Yamasaki, S. Akira, F. Gantner, and K.B. Bacon. 2004. Essential role of MHC II-independent CD4+ T cells, IL-4 and STAT6 in contact hypersensitivity induced by fluorescein isothiocyanate in the mouse. *Int. Immunol.* 16:685–695.
34. Suto, H., S. Nakae, M. Kakurai, J.D. Sedgwick, M. Tsai, and S.J. Galli. 2006. Mast cell-associated TNF promotes dendritic cell migration. *J. Immunol.* 176:4102–4112.
35. Wershil, B.K., T. Murakami, and S.J. Galli. 1988. Mast cell-dependent amplification of an immunologically nonspecific inflammatory response. Mast cells are required for the full expression of cutaneous acute inflammation induced by phorbol 12-myristate 13-acetate. *J. Immunol.* 140:2356–2360.
36. Martin, T.R., T. Takeishi, H.R. Katz, K.F. Austen, J.M. Drazen, and S.J. Galli. 1993. Mast cell activation enhances airway responsiveness to methacholine in the mouse. *J. Clin. Invest.* 91:1176–1182.
37. Bulanova, E., V. Budagian, Z. Orinska, M. Hein, F. Petersen, L. Thon, D. Adam, and S. Bulfone-Paus. 2005. Extracellular ATP induces cytokine expression and apoptosis through P2X7 receptor in murine mast cells. *J. Immunol.* 174:3880–3890.
38. Lau, E.K., S. Allen, A.R. Hsu, and T.M. Handel. 2004. Chemokine-receptor interactions: GPCRs, glycosaminoglycans and viral chemokine binding proteins. *Adv. Protein Chem.* 68:351–391.
39. Hata, D., Y. Kawakami, N. Inagaki, C.S. Lantz, T. Kitamura, W.N. Khan, M. Maeda-Yamamoto, T. Miura, W. Han, S.E. Hartman, et al. 1998. Involvement of Bruton's tyrosine kinase in FcεRI-dependent mast cell degranulation and cytokine production. *J. Exp. Med.* 187:1235–1247.
40. Fleming, T.J., E. Donnadieu, C.H. Song, F.V. Laethem, S.J. Galli, and J.P. Kinet. 1997. Negative regulation of FcεRI-mediated degranulation by CD81. *J. Exp. Med.* 186:1307–1314.
41. Wise, A., S.C. Jupe, and S. Rees. 2004. The identification of ligands at orphan G-protein coupled receptors. *Annu. Rev. Pharmacol. Toxicol.* 44:43–66.
42. Bauer, M., V. Redecke, J.W. Ellwart, B. Scherer, J.P. Kremer, H. Wagner, and G.B. Lipford. 2001. Bacterial CpG-DNA triggers activation and maturation of human CD11c-, CD123+ dendritic cells. *J. Immunol.* 166:5000–5007.
43. Tono, T., T. Tsujimura, U. Koshimizu, T. Kasugai, S. Adachi, K. Isozaki, S. Nishikawa, M. Morimoto, Y. Nishimune, S. Nomura, et al. 1992. c-kit Gene was not transcribed in cultured mast cells of mast cell-deficient Wsh/Wsh mice that have a normal number of erythrocytes and a normal c-kit coding region. *Blood.* 80:1448–1453.
44. Ponath, P.D., S. Qin, T.W. Post, J. Wang, L. Wu, N.P. Gerard, W. Newman, C. Gerard, and C.R. Mackay. 1996. Molecular cloning and characterization of a human eotaxin receptor expressed selectively on eosinophils. *J. Exp. Med.* 183:2437–2448.
45. Palermo, D.P., M.E. DeGraaf, K.R. Marotti, E. Rehberg, and L.E. Post. 1991. Production of analytical quantities of recombinant proteins in Chinese hamster ovary cells using sodium butyrate to elevate gene expression. *J. Biotechnol.* 19:35–47.
46. Livak, K.J., and T.D. Schmittgen. 2001. Analysis of relative gene expression data using real-time quantitative PCR and the 2(-Delta Delta C(T)) Method. *Methods.* 25:402–408.
47. Liu, F.T., J.W. Bohn, E.L. Ferry, H. Yamamoto, C.A. Molinaro, L.A. Sherman, N.R. Klinman, and D.H. Katz. 1980. Monoclonal dinitrophenyl-specific murine IgE antibody: preparation, isolation, and characterization. *J. Immunol.* 124:2728–2737.
48. Wershil, B.K., Z.S. Wang, J.R. Gordon, and S.J. Galli. 1991. Recruitment of neutrophils during IgE-dependent cutaneous late phase reactions in the mouse is mast cell-dependent. Partial inhibition of the reaction with antiserum against tumor necrosis factor-alpha. *J. Clin. Invest.* 87:446–453.